

Si(100)-(2×1) surface defects and dissociative and nondissociative adsorption of H₂O studied with scanning tunneling microscopy

M. Chander, Y. Z. Li, J. C. Patrin, and J. H. Weaver

Department of Materials Science and Chemical Engineering, University of Minnesota, Minneapolis, Minnesota 55455

(Received 8 September 1992)

We have investigated the adsorption characteristics of H₂O on Si(100)-(2×1) at 300 K using scanning tunneling microscopy. Nondissociative adsorption is shown to occur at low coverage, as characterized by the formation of dark features in both occupied- and unoccupied-state images. Such features form straight chains, termed *W* defects, derived from two to six H₂O molecules. The *C*-type defects commonly observed on Si(100)-(2×1) are shown to be identical to *W* defects with two H₂O molecules. These results also show that most of the dark dimer features on Si(100)-(2×1) result from H₂O adsorption, i.e., they are not dimer vacancies. Dissociative adsorption is observed at higher exposure. It is characterized by two-dimensional patches where Si—H and Si—OH states can be resolved as atomic features of different intensities. A 2×1 structure consisting of Si—H and Si—OH is observed at saturation, but there is no long-range order in the arrangement of H and OH. Through saturation, there is also evidence of oxidation.

INTRODUCTION

Wet oxidation processes are of great importance to the electronic-devices industry.^{1–6} Not surprisingly, the adsorption characteristics of H₂O on Si surfaces have been the topic of much study. Two forms of adsorption have been suggested for the saturated surface, namely dissociative and nondissociative. The infrared (IR) spectroscopy study of Chabal and Christman⁴ convincingly showed that water chemisorbs dissociatively to form H and OH on Si(100)-(2×1) for saturation exposures at 300 K. While the adsorption characteristics have been revealed for the saturated surface, much less is known about H₂O-induced electronic and geometric structures at sub-monolayer coverages. Since this regime is important for understanding the mechanisms of surface modification, either from intentional dosing or from residual H₂O in the vacuum system, we were motivated to undertake a scanning tunneling microscopy (STM) study of H₂O on Si(100).

In this paper, we present STM results for H₂O adsorption on Si(100)-(2×1) at 300 K, starting at low coverage and extending to saturation. The low-coverage regime is characterized by the nondissociative adsorption of H₂O with features that are identical to the *C*-type defects routinely found on “clean” surfaces.^{7,8} These defects link into chains, termed *W* (water-induced) defects. Dark dimer features, denoted *M*, are also formed during nondissociative adsorption. These have previously been attributed to missing dimers on the clean surface but their development during H₂O adsorption implies that not all dark dimer features are missing dimers. Clusters of dark features, termed cluster defects, also form during nondissociative adsorption. They can be analyzed as groups of *W* and *M* features, but they do not show dimer or atomic resolution. Increased H₂O exposure gives rise to a second mode of adsorption characterized by two-

dimensional patches. These patches appear to have nucleated on the *W*, *M*, and cluster features, but they differ from them in that atomic resolution is possible. In particular, two different intensities of brightness are evident and we attribute them to dissociated H and OH bonded to Si, as suggested by IR (Ref. 4) and electron-energy-loss spectroscopy⁵ (EELS) studies. The saturated overlayer exhibits a 2×1 structure that consists mostly of the dissociated H and OH species with some indication of oxide formation.

EXPERIMENT

The STM experiments were conducted using a Park Scientific microscope⁹ in an ultrahigh-vacuum chamber. We used polished *p*-type Si wafers (B-doped, resistance <0.01 Ω cm that were oriented to within 0.5° of (100). The wafers were ultrasonically cleaned using ethanol before introduction into the STM chamber. Degassing was done *in situ* at ~600°C overnight, followed by flashing to ~1200°C for 1 min to remove the oxide layer and then cooling to ~600°C over a period of 2–3 min. This procedure has been shown to give clean, well-ordered Si(100)-(2×1) surfaces.¹⁰

Deionized water was purified using several freeze-pump-thaw cycles. Dosing was done through a leak valve at 5×10⁻¹⁰ Torr. Exposures were measured using an ion gauge that was not in the direct line of sight with the sample. Residual gas analysis of the chamber showed a partial pressure of H₂O of 2×10⁻¹¹ Torr at the chamber base pressure of 7×10⁻¹¹ Torr. Several studies were conducted that explored the effects of condensation of H₂O from the residual gas background, and these studies demonstrated that residual gas dosing gave the same results as intentional dosing. That such unintentional dosing mainly led to H₂O adsorption on the surface is evident from analysis of the residual gas spectrum. The percentages of the residual gases relative to H₂O (at base

pressure) were $\sim 60\%$ H_2 , 50% CO , 25% H , and negligible CO_2 . During intentional dosing, the H_2O partial pressure in the chamber was at least eight times higher than the others. Adsorption of H_2 , CO , and CO_2 can be neglected on account of their low sticking coefficients compared to H_2O and H .¹¹ Even though H has a high sticking coefficient [~ 0.4 L (1 L = 10^{-6} Torr s) room-temperature (RT) dose of H_2 in the presence of a 1800-K W filament saturates $\sim 30\%$ of the Si(111)-(7 \times 7) surface],¹² its partial pressure is too small to account for the features observed as a result of residual gas adsorption. Finally, H_2O has a sticking coefficient of nearly unity,¹ therefore its adsorption is highly favored. The contamination of the Si(100)-(2 \times 1) surface by residual H_2O over a period of ~ 30 min at 2×10^{-10} Torr (base pressure) has been noted previously by Chabal.¹³

RESULTS

Symmetric and asymmetric dimers of the clean surface

STM images of the occupied and unoccupied states of Si(100)-(2 \times 1) are shown in Figs. 1(a) and 1(b), respectively. These were acquired simultaneously on the same region of the clean surface. Figures 1(c) and 1(d) are schematic representations of Figs. 1(a) and 1(b). The STM images are typical of results in the literature,^{7,8,10,14} and they represent the starting conditions for the H_2O adsorption studies. Rows of dimers can be seen in both images. Symmetric dimers, labeled S , appear as single bright protrusions centered on the dimer rows in Figs. 1(a) and 1(c). It is believed that dimers buckle into two tilt directions^{8,15-17} separated by an energy barrier that is comparable to thermal energy at room temperature. Hence, the dimers fluctuate on a time scale that is small compared to the imaging time¹⁷ and they appear to be symmetric. One buckling direction is stabilized near defects,^{7,8,14} producing a dipole where the up atom is slightly negative compared to the down atom.¹⁸ The resulting asymmetric dimers, labeled A , appear as protrusions centered on one of the atoms of the dimers in Figs. 1(a) and 1(c). Adjacent A features in the same row tend to buckle in opposite directions (anticorrelated buckling) due to elastic strain and Coulomb potential interactions.^{8,19} Such zig-zag A 's are evident in Figs. 1(a) and 1(c).

In the time-averaged symmetric configuration, the unoccupied dimer- π states that participate in tunneling have nodes at the centers of dimers and maxima at their ends.²⁰ Consequently, the dimers can be resolved into two atoms in unoccupied-state images. The asymmetric nature of the dimers in Figs. 1(a) and 1(c) is not as evident in Figs. 1(b) and 1(d). This is possibly due to the combined effect of the local density of states of the dimers and the Coulomb interaction of the tip with the dimers^{17,19} since we have observed asymmetric dimers in unoccupied-state images under certain biasing conditions.

Defects of the clean surface

Figures 1(a) and 1(c) show features, labeled W , that occupy a unit cell each and have a dark site adjacent to a

bright site (we use W to indicate that they are water related). The bright sites and the dark sites of adjacent W 's line up to form straight chains. Although asymmetric dimers also appear as a set of dark and bright sites, the bright sites of such dimers form zig-zag chains. W features rarely exist as single isolated features. Most are found as chains of two, typically known as C -type defects,⁷ as shown in Figs. 1(a) and 1(c). These defects induce buckling in dimers around them.^{7,8} For example, the zig-zag chain of A 's in Fig. 1(a), outlined in Fig. 1(c), arises from the C -type defect at its lower end.

In the unoccupied states, the W features appear as a set of bright and dark atomic features, as shown in Figs. 1(b) and 1(d).⁷ It is evident that the bright features in W in the occupied-state image overlap with the bright features in the unoccupied-state image and the same is true for the dark features. However, in the unoccupied-state images, the bright features show much more bias dependence in their apparent heights than in the occupied-state images.

Although the C -type defects are the most abundant of the W features on a typical clean surface, chains of up to five W features have been observed. A chain of three W 's is marked in the upper right portion in Fig. 1. We note that published images of clean Si(100) show W chains as well as C -type defects.^{7,8,14} In the next section, we argue that C and W features are produced by H_2O adsorption.

Figure 1 shows features that appear dark in the occupied- and the unoccupied-state images and are also a unit cell in size. These features, labeled M , have been attributed historically to missing dimers. Analysis of clean surface results shows that they can account for 5–8% of the surface.^{7,8,14} In contrast to the W features, the M features do not induce buckling in adjacent dimers, as depicted in Figs. 1(a) and 1(c).⁷ It is argued below that they are produced by nondissociative adsorption of two H_2O molecules per dimer.

Low H_2O exposures and growth of W and M defects

Figure 2(a) shows a typical STM image of the occupied states after exposure to 0.05 L of H_2O (1 L = 1×10^{-6} Torr s). This is equivalent to a coverage of ~ 0.05 (ML) since the sticking coefficient is unity.¹ Comparison to the clean surface shows a marked increase in the number of dark features. While several can be identified as belonging to W chains and M features, the remainder appear in clusters, termed cluster defects CD. More than 95% of the cluster defects can be characterized as groups of W - and M -type features. For example, the CD in area 1 of Fig. 2(a) is a grouping of two chains, each consisting of four W 's. The cluster defect in area 2 is a chain of two W 's terminated by an M . Quantitatively, the number of dark features in W chains has nearly doubled from 3–4% for the clean surface to 6–7% after exposure to 0.05 L H_2O .

Water adsorption at low exposures also produces M features. We believe that an M feature arises from two dark features per surface unit cell, thus making the whole unit cell dark, in contrast to a W feature where only half of the unit cell is dark. Thus, the number of dark features in M 's (two per M) have increased from 4–5%

to 6–7% after 0.05 L exposure. The total increase in the number of dark features in *W*'s and *M*'s (~5%) correlates well with 0.05 ML H₂O chemisorbed on the surface. This is indicative of nondissociatively adsorbed H₂O if we attribute each dark feature to a molecule bonded to a Si atom. (The reason for the association of these features to nondissociatively adsorbed H₂O instead of dissociative H or OH will be clearer in the next section.)

Previous STM studies of Si(100)-(2×1) have interpreted the *M* features as dimer vacancies.^{7,8,14} The above analysis implies that not all such features are genuine vacancies. Unfortunately, all of the *M* features appear identical in the occupied- and the unoccupied-state images and we cannot distinguish H₂O-related *M* features from true missing dimers. Evidence that two inequivalent *M*-type features do exist can be found in the saturated surface (discussed below) because a fraction of the *M* features persist.

The implication that a substantial fraction of *M*

features of clean surfaces are H₂O related is plausible given the fact that there is residual water vapor in every vacuum system and that imaging of a freshly cleaned Si wafer is typically done on a time scale of hours. If the operating pressure is 2×10^{-10} Torr and the H₂O partial pressure is 5×10^{-11} Torr, then an unintentional dose equivalent to saturation, 0.5 L, is achieved in ~3 h. A confirmation of this was obtained by studying the time evolution of the clean surface at 7×10^{-11} Torr where residual gas analysis showed an H₂O partial pressure of $\sim 2 \times 10^{-11}$ Torr. Both *M* and *W* features were found to increase with time and the progression was similar *in all aspects* to that obtained by deliberate H₂O dosing. Finally, studies done subsequent to those under analysis here showed a marked decrease in the number of “missing dimer” features on a freshly cleaned wafer, although the only parameter changed during surface preparation was the base pressure (the number of missing dimer features was ~2% when the base pressure was 4×10^{-11} Torr).

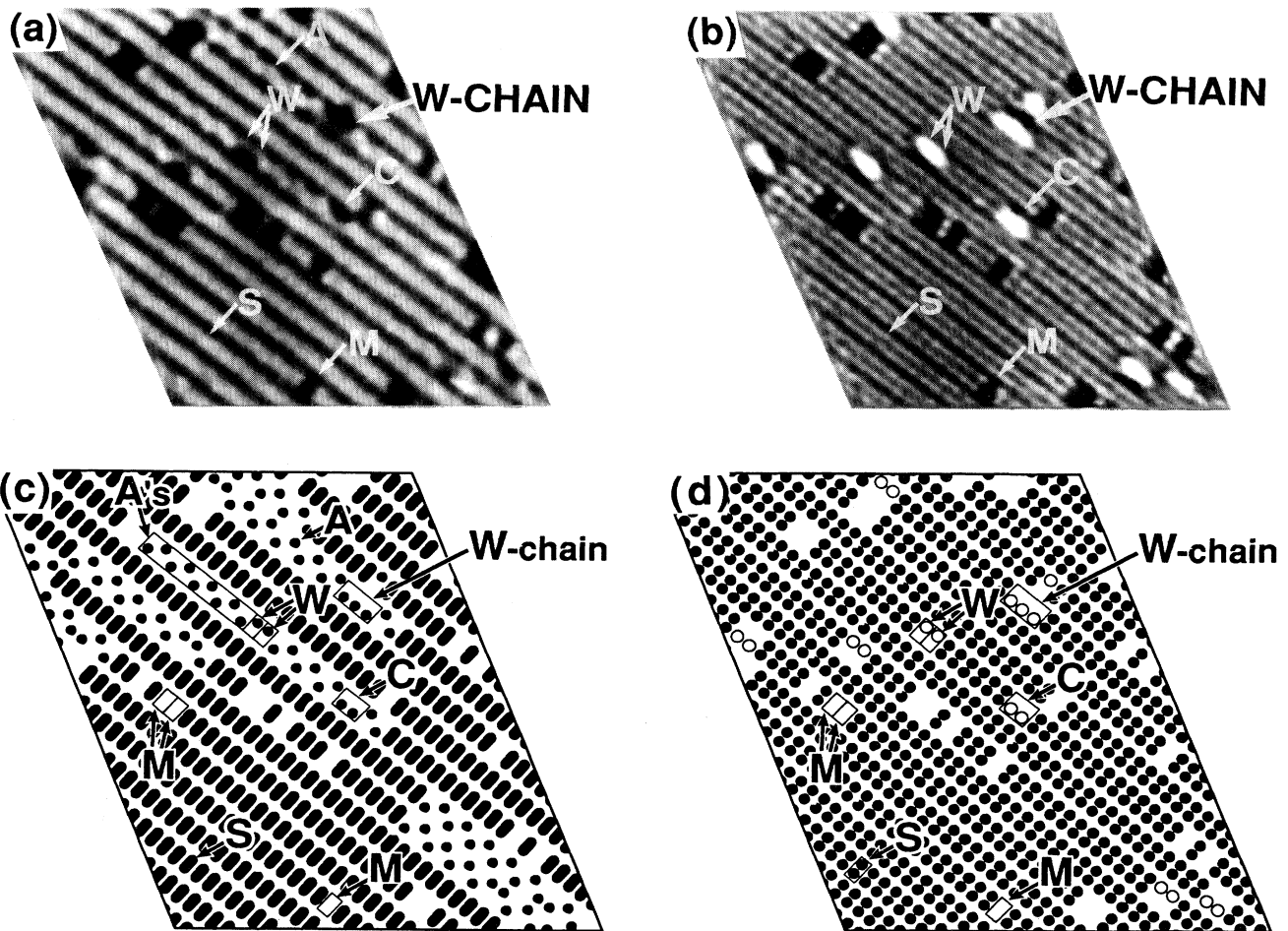


FIG. 1. Drift-corrected, curvature-enhanced STM images of (a) the occupied states and (b) the unoccupied states of the same region of the clean Si(100)-(2×1) surface (± 1.3 -V bias). (c) and (d) are schematics of the same region, showing only the top atomic layer. *S* and *A* denote symmetric and asymmetric dimers, *M* points to a dark dimer, *W* represents an H₂O-attached dimer, and *C* draws attention to a defect with two *W*'s.

Dissociative chemisorption at higher H₂O exposures

Increasing the exposure of Si(100)-(2×1) to 0.1 ML H₂O produced two-dimensional patches that are indicative of extended adsorbate-adsorbate interaction. Imaging within the patches showed that the dimers could be resolved into two atomic features in occupied-state images, in contrast to the behavior at low coverage, suggesting H₂O dissociation. Exposure to 0.2 ML H₂O further increased the number of dimers having atomic resolution. Moreover, these atomic features had different intensities, as seen in the occupied-state image of Fig. 2(b). For example, two of the atoms in the outlined unit cells appear larger than the other two. The association of these

features with Si—H and Si—OH states is based on the conclusions of IR (Ref. 4) and EELS (Ref. 5) studies. Note that this evolution from nondissociative to dissociative chemisorption does not contradict the results from vibrational spectroscopy studies because those techniques were not sensitive to low amounts of molecular water.¹

Most of the bright protrusions in Fig. 2(b) are unreacted dimers. Although *W* and *M* features are still visible, their number has been reduced significantly. This implies that some of the *W* and *M* features have converted into dissociated species. The lack of atomic resolution in the features formed in the low exposure regime is indicative of an adsorption mode that is different from the dissociative mode. Since the only other plausible pathway for ad-

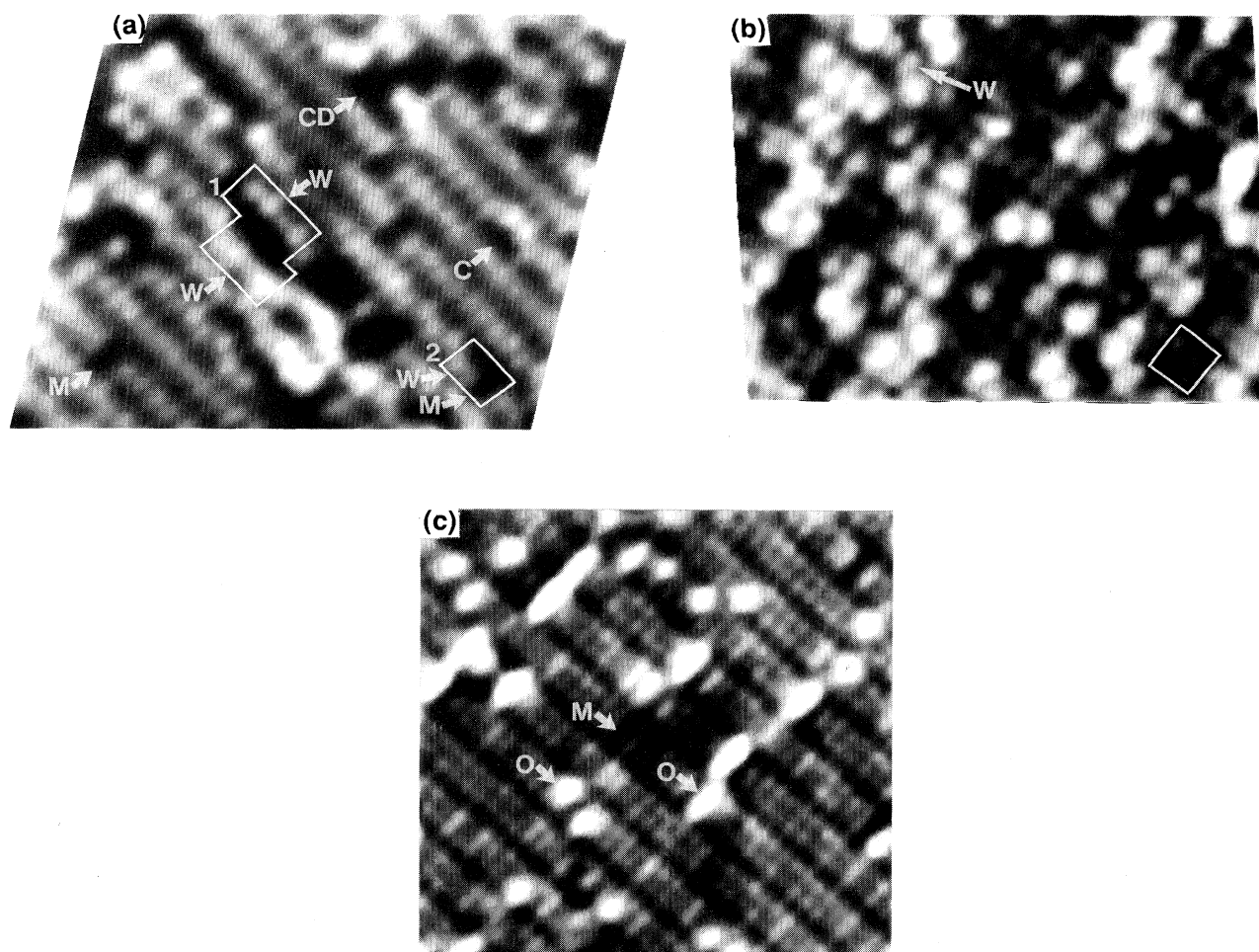


FIG. 2. (a) Drift-corrected occupied-states image of Si(100)-(2×1) after 0.05 L H₂O exposure (sample bias -1.79 V). Comparison to Fig. 1 shows that H₂O adsorption produces dark features that appear as isolated *M* and *W* features, as well as cluster defects (CD) derived from groups of *W*'s and *M*'s. The *W*'s and some of the *M*'s are related to adsorbed H₂O, with each dark atomic feature representing one molecule bonded to a Si atom. (b) Occupied-state image obtained after 0.2 L H₂O exposure (sample bias -2.01 V). Atomic resolution of the dimers is now possible on a substantial portion of the surface but it was not possible on the clean surface. Atoms within the two 2×1 unit cells outlined in the bottom exhibit different intensities of brightness that are attributed to Si—H and Si—OH states. Most of the bright features are unreacted. *W* and *M* features are also recognizable. (c) Occupied-state image of the saturated Si(100)-(2×1) surface after 0.5 L H₂O exposure (sample bias -1.61 V). Most of the dimers can be atomically resolved. The different intensities within a dimer reflect Si—H and Si—OH bonding but there is no long-range ordering of these species. Bright atomic protrusions marked *O* reflect oxidation. The dark *M* features appear to be dimer vacancies that remain unreacted.

sorption of H₂O is nondissociative under the given conditions, we believe that the *W* features, the *M* features, and the cluster defects arise from nondissociative chemisorption of water.

H₂O exposure above 0.2 ML produces more features that have been assigned to Si—H and Si—OH bonds. Ultimately, a 2×1 overlayer is evident from the occupied-states image of Fig. 2(c) for the saturated surface. The persistence of a dimerized structure implies that the Si(100) surface has not been disrupted. While most dimers show atomic resolution, there is no long-range order in the arrangement of features with different intensities.

Figure 2(c) shows bright protrusions on the saturated surface labeled *O*. Some of these appear localized on single atoms whereas others appear straddling the dimers. Their apparent heights range between 0.5 and 1.2 Å, depending on the sample bias. We suspect that they are related to Si oxidation, consistent with the results of a photon-stimulated desorption study of Larsson *et al.*²¹ where small amounts of oxide were detected at saturation. Their density is relatively independent of the density of dimer vacancies on the starting surface and we found no evidence that they form on missing dimers. The *O* features remain unchanged when the surface is exposed to five times the saturation exposure, implying that they are not unreacted Si atoms. The similarity in appearance of the *O* features in Fig. 2(c) and bright features in Fig. 2(b) suggests that *O* features may have formed prior to saturation so that oxidation offers an alternate channel to H₂O dissociation and chemisorption.

Images like those of Fig. 2(c) show that ~1% of the saturated surface is still derived from *M* features. Hence, most of the *M*-type features imaged at low exposure were converted into dissociated species, consistent with them being derived from Si—H₂O rather than missing dimers. Those that persist at saturation persist at increased exposures. These features have the same appearance regardless of whether they are present in the vicinity of the *O* features or away from them. Hence, we speculate that these passive *M* features are related to intrinsic dimer vacancies.

Figure 3 shows images of the saturated surface obtained simultaneously at ±2.6 V bias. The atomically resolved 2×1 structure, evident in the occupied-state image, is absent in the unoccupied-state image. This is unlike the behavior of (2×1) Si—H where the 2×1 structure is evident in both the occupied and unoccupied state images.²⁰ This indicates that Si—H and Si—OH states above *E_F* accessed by the tunneling tip have a delocalized nature. Since imaging of the unoccupied states was possible only with sample biases exceeding ~2 V, we conclude that there are no states between *E_F* and +2 eV for the saturated surface. This is in sharp contrast to the low exposure behavior where the water-related features gave rise to states close to *E_F*.

The dark regions in the outlined regions 1–3 in the unoccupied-state image of Fig. 3 are associated with the bright *O* features in the occupied-state image. Moreover, the transitions are abrupt from dark regions of the unoccupied-state image to the brighter areas around them. These abrupt transitions could reflect changes in

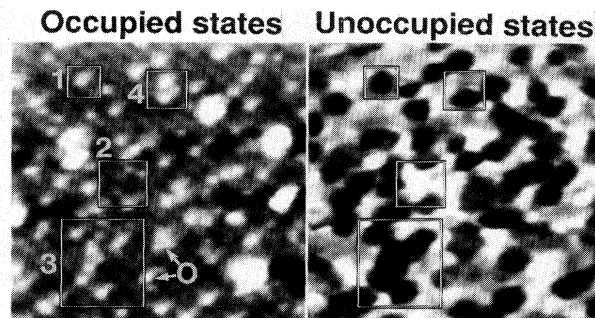


FIG. 3. Simultaneously acquired images of the occupied states and the unoccupied states of the saturated surface (sample bias ±2.6 V, 150×150 Å²). The absence of atomic resolution in the unoccupied-state image implies that the empty Si—H and Si—OH states are delocalized. The dark depressions in the unoccupied-state image correspond to the *O* or oxide features in the occupied-state image. The abrupt transition between light and dark areas may represent electron trapping sites around the oxide features.

the state density but they are more likely to arise from sites of enhanced electron trapping. Such trapping is suggested by the Si(100) oxidation work of Koch and Hamers²² where STM images revealed that circular depressions, the edges of which acted as electron trapping sites, appeared after oxidation with a monolayer-equivalent of molecular oxygen. Detailed comparison of the images in Fig. 3 shows that the bright *O* features are not all alike chemically. For example, some of the bright features outlined in region 4 in the occupied-state image remain bright in the unoccupied-state image whereas the others appear dark. This may indicate different stages of oxidation.

DISCUSSION

Nondissociative H₂O—Si bonding is expected to involve charge transfer from the lone pair orbitals of O to Si, as for molecular adsorption on most metals.¹ This is consistent with the work function decrease around *C*-type defects.⁷ Figure 4 depicts the proposed bonding geometry. The presence of one empty dangling bond per Si atom implies attachment of one H₂O molecule. Water attachment with its O lone pair will be favored at the down atom. This deepens the potential well of one tilt direction over the other and stabilizes the neighboring buckled dimers. Adsorption of alkali metals on Si(100), which also involves charge transfer to the substrate, shows a similar stabilization of buckled dimers.^{23,24}

The formation of chainlike features at low coverage indicates that H₂O molecules are mobile on the surface at 300 K.²⁵ Since single dark features are rare, it is likely that bimolecular units are the first stable structures, i.e., the *C*-type defects. Stability is achieved by establishing two bonds per water molecule, namely, an oxygen lone pair bond with the substrate and a hydrogen bond with an adjacent molecule. With typical hydrogen bond energies of ~0.3 eV per molecule,¹ such units are substantially more stable than single H₂O molecules. The chains

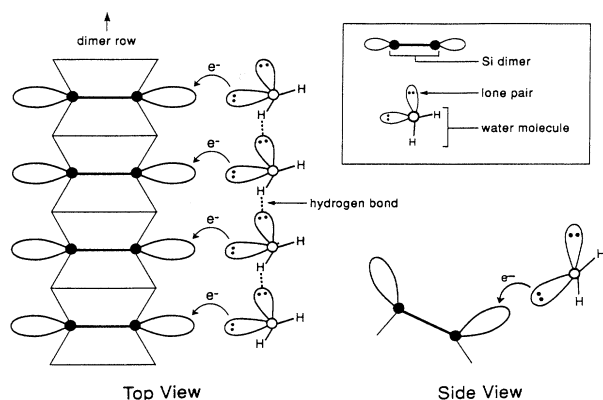


FIG. 4. Sketches of a W chain derived from four H_2O molecules attached to dimer atoms in a row. The bonding of H_2O to Si involves charge transfer from the lone pair orbitals of O to Si empty dangling bonds. The chain of water molecules is stabilized by intermolecular hydrogen bonds.

grow with the addition of more H_2O . One such chain of four water molecules is depicted in the model in Fig. 4. This model is consistent with adsorption structures for nondissociative adsorption on metal surfaces where each molecule in a stable structure needs a minimum of two bonds.¹ The dark M -type features would then have both hydrogen-bonded water molecules on the same dimer.

The observation of straight H_2O chains and the assumption that H_2O attaches to the down atoms would indicate that adjacent dimers prefer to buckle in the same direction in the presence of H_2O . This is then in contrast to anticorrelated buckling favored by asymmetric dimers in the absence of H_2O . Energy reduction can be achieved via the hydrogen bond between adjacent H_2O molecules. Hence, the structure of H_2O chains is believed to be determined by an interplay between the coupling energy for anticorrelated buckling and the hydrogen bond energy between H_2O attached to adjacent dimers. Thus, the formation of straight chains would indicate that the anticorrelated buckling energy is less than the hydrogen bond energy (~ 0.3 eV). Note that the hydrogen bond

strength for anticorrelated dimers is significantly reduced relative to correlated dimers because of the increased O—H distance.¹

We speculate that the thermodynamically favored transition from nondissociative to dissociative bonding is accomplished by a cooperative modification of the local substrate structure. In the absence of such a cooperative effect, the H_2O molecules remain stable. Since W defects stabilize the buckling of nearby dimers, two such W defects can alter the structure of intervening dimers depending on whether their buckling effects are in phase or out of phase.⁸ We speculate that some of the buckled dimers cannot change their buckling direction to accommodate new H_2O molecules in the chains when the local density of W defects exceeds a critical value. Hence, stable dipoles are produced. Polar H_2O molecules that arrive at these stable dimeric dipoles now experience a strong interaction between OH and the down atom, and H and the up atom,²⁶ and dissociate. A strong interaction between H_2O and the substrate is predicted to be essential for the reduction of the dissociation barrier from gas phase values of ~ 5 eV/molecule to as low as ~ 0.5 eV/molecule and the consequent stabilization of dissociation fragments in the case of adsorption on metals.¹

This study has explored the nature of defects commonly found on clean Si(100)- 2×1 and the relationship of these defects to H_2O adsorption. The evidence supports that W -type defects can arise from chains of H_2O molecules; a chain of two molecules is the stable C -type defect commonly observed. Significantly, a majority of the dark features observed on clean surfaces that have been referred to as missing dimers are directly related to nondissociative H_2O chemisorption. Some of these dark features remain unreacted throughout the adsorption process; their lack of reaction probably indicates that they are true missing dimers and are relatively inert. We have shown that the barrier for dissociation of H_2O is large on the clean surface. The formation of H_2O chains and the stabilization of dimeric dipoles appear to be important precursors for dissociative chemisorption.

ACKNOWLEDGMENTS

This work was supported by IST/SDIO and managed by the Office of Naval Research.

¹See, for example, the exhaustive review by P. A. Thiel and T. E. Madey, *Surf. Sci. Rep.* **7**, 211 (1987) and references therein.
²K. Fujiwara, *Surf. Sci.* **108**, 124 (1981); *J. Chem. Phys.* **75**, 5172 (1981); K. Fujiwara and H. Ogata, *Surf. Sci.* **86**, 700 (1979).
³D. Schmeisser, F. J. Himpsel, and G. Hollinger, *Phys. Rev. B* **27**, 7813 (1983); D. Schmeisser, *Surf. Sci.* **137**, 197 (1984).
⁴Y. J. Chabal and S. B. Christman, *Phys. Rev. B* **29**, 6974 (1984).
⁵H. Ibach, H. Wagner, and D. Bruchmann, *Solid State Commun.* **42**, 457 (1982); H. Ibach, H. D. Bruchmann, and H. Wagner, *Appl. Phys. A* **29**, 113 (1982); J. A. Schaefer, F. Stucki, D. J. Frankel, W. Göpel, and G. J. Lapereyre, *J. Vac. Sci. Technol. B* **2**, 359 (1984).

⁶S. Ciraci and H. Wagner, *Phys. Rev. B* **27**, 5180 (1983).
⁷R. J. Hamers and U. K. Köhler, *J. Vac. Sci. Technol. A* **7**, 2854 (1989).
⁸R. A. Wolkow, *Phys. Rev. Lett.* **68**, 2636 (1992).
⁹Park Scientific Instruments, Mountain View, CA.
¹⁰B. S. Swartzentruber, Y.-W. Mo, M. B. Webb, and M. G. Lagally, *J. Vac. Sci. Technol. A* **7**, 2901 (1989).
¹¹E. Ekwelundu and I. Ignatiev, *Surf. Sci.* **179**, 119 (1987); S. Tougaard, P. Morgen, and J. Onsgaard, *ibid.* **111**, 545 (1981); B. A. Joyce and J. H. Neave, *ibid.* **34**, 401 (1973).
¹²J. J. Boland, *Phys. Rev. Lett.* **65**, 3325 (1990).
¹³Y. J. Chabal, *Phys. Rev. B* **29**, 3677 (1984).
¹⁴See, for example, R. M. Tromp, R. J. Hamers, and J. E. Demuth, *Phys. Rev. Lett.* **55**, 1303 (1985); R. J. Hamers, R.

- M. Tromp, and J. E. Demuth, *Phys. Rev. B* **34**, 5343 (1986).
- ¹⁵N. Roberts and R. J. Needs, *Surf. Sci.* **236**, 112 (1990).
- ¹⁶R. J. Hamers, R. M. Tromp, and J. E. Demuth, *Surf. Sci.* **181**, 346 (1987).
- ¹⁷J. Dabrowski and M. Scheffler, *Appl. Surf. Sci.* **56**, 15 (1992).
- ¹⁸J. Ihm, M. L. Cohen, and D. J. Chadi, *Phys. Rev. B* **21**, 4592 (1980); D. J. Chadi, *Phys. Rev. Lett.* **43**, 43 (1979).
- ¹⁹G. P. Kochanski and J. E. Griffith, *Surf. Sci.* **249**, L293 (1991).
- ²⁰R. J. Hamers, Ph. Avouris, and F. Bozso, *Phys. Rev. Lett.* **59**, 2071 (1987).
- ²¹C. U. S. Larsson, A. S. Flodström, R. Nyholm, L. Incoccia, and F. Senf, *J. Vac. Sci. Technol. A* **5**, 3321 (1987).
- ²²R. H. Koch and R. J. Hamers, *Surf. Sci.* **181**, 333 (1987).
- ²³M. Tsuda, T. Hoshino, S. Oikawa, and I. Ohdomari, *Phys. Rev. B* **44**, 11 241 (1991).
- ²⁴T. Hashizume, Y. Hasegawa, I. Kamiya, T. Ide, I. Sumita, S. Hyodo, T. Sakurai, H. Tochihara, M. Kubota, and Y. Murata, *J. Vac. Sci. Technol. A* **8**, 233 (1990).
- ²⁵While the activation energy for diffusion is not known, diffusion barriers are typically 10% to 40% of adsorbate desorption energies (Ref. 1). Typical bond energies for non-dissociative chemisorption of H₂O are roughly -0.5 eV/molecule (Ref. 1). Assuming the upper limit of 40%, we obtain a diffusion barrier of 0.2 eV, consistent with facile diffusion.
- ²⁶J. Q. Broughton, J. A. Schaefer, J. C. Bean, and H. H. Farrell, *Phys. Rev. B* **33**, 6841 (1986).

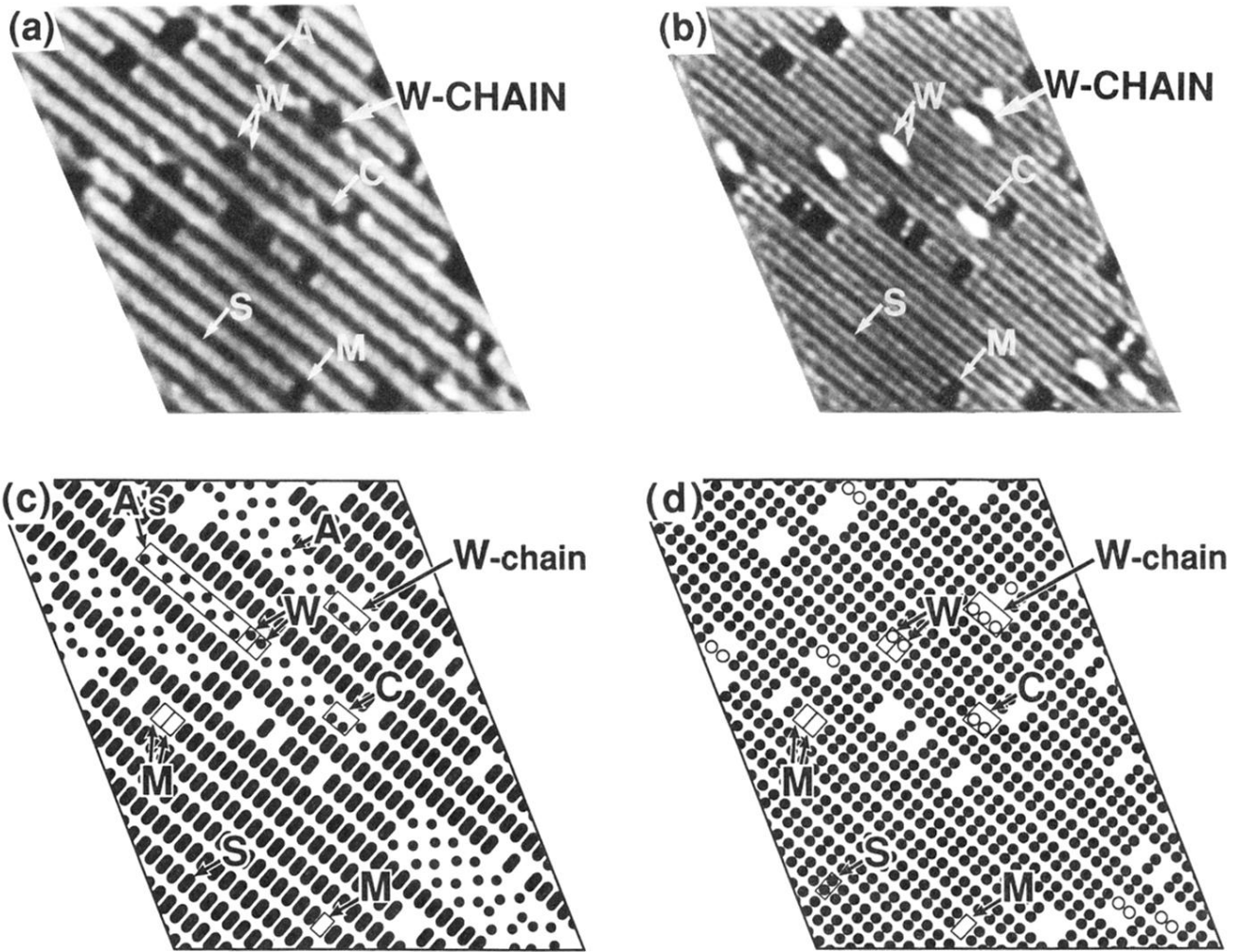


FIG. 1. Drift-corrected, curvature-enhanced STM images of (a) the occupied states and (b) the unoccupied states of the same region of the clean Si(100)-(2×1) surface (± 1.3 -V bias). (c) and (d) are schematics of the same region, showing only the top atomic layer. *S* and *A* denote symmetric and asymmetric dimers, *M* points to a dark dimer, *W* represents an H₂O-attached dimer, and *C* draws attention to a defect with two *W*'s.

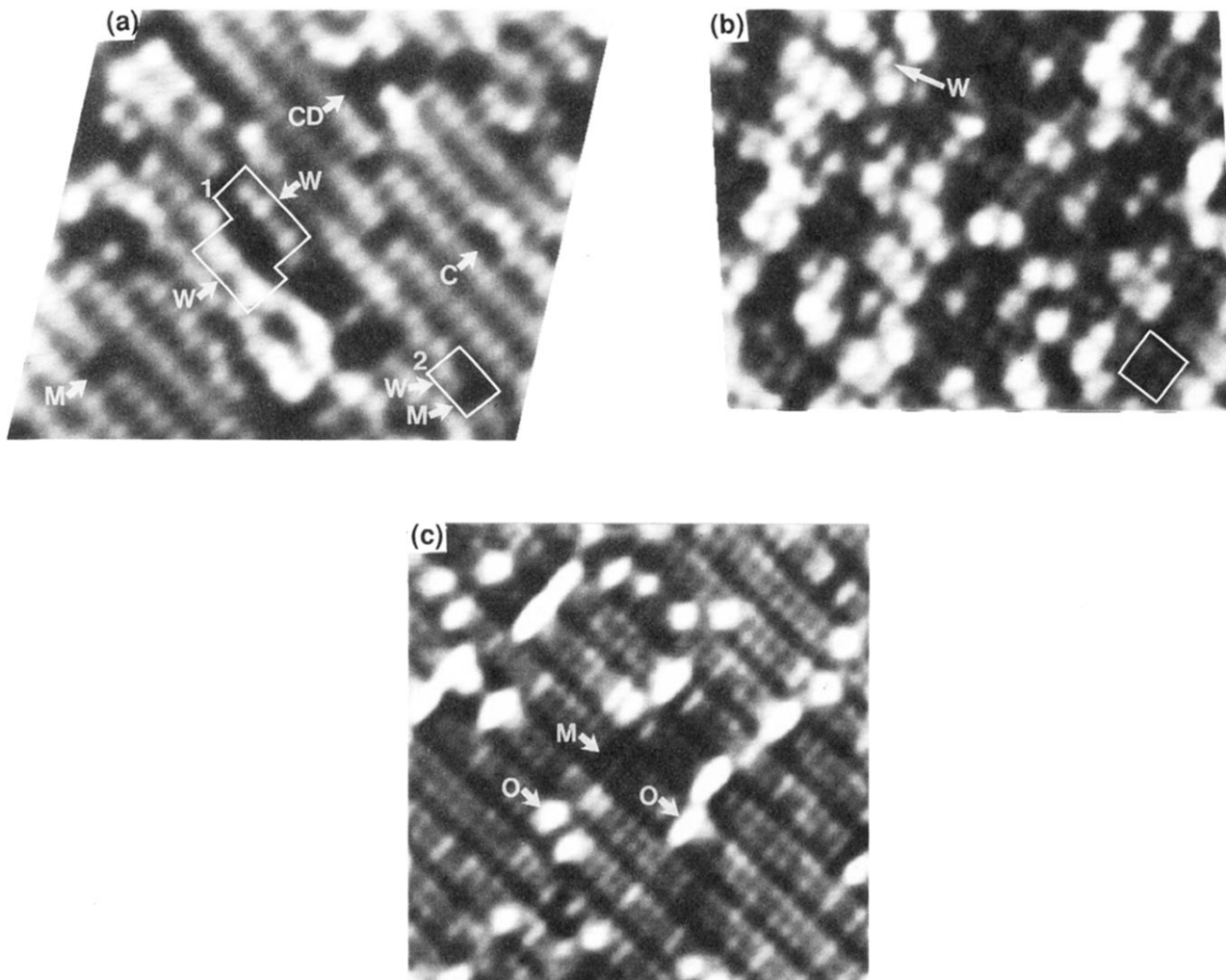


FIG. 2. (a) Drift-corrected occupied-states image of Si(100)-(2 \times 1) after 0.05 L H₂O exposure (sample bias -1.79 V). Comparison to Fig. 1 shows that H₂O adsorption produces dark features that appear as isolated *M* and *W* features, as well as cluster defects (CD) derived from groups of *W*'s and *M*'s. The *W*'s and some of the *M*'s are related to adsorbed H₂O, with each dark atomic feature representing one molecule bonded to a Si atom. (b) Occupied-state image obtained after 0.2 L H₂O exposure (sample bias -2.01 V). Atomic resolution of the dimers is now possible on a substantial portion of the surface but it was not possible on the clean surface. Atoms within the two 2 \times 1 unit cells outlined in the bottom exhibit different intensities of brightness that are attributed to Si-H and Si-OH states. Most of the bright features are unreacted. *W* and *M* features are also recognizable. (c) Occupied-state image of the saturated Si(100)-(2 \times 1) surface after 0.5 L H₂O exposure (sample bias -1.61 V). Most of the dimers can be atomically resolved. The different intensities within a dimer reflect Si-H and Si-OH bonding but there is no long-range ordering of these species. Bright atomic protrusions marked *O* reflect oxidation. The dark *M* features appear to be dimer vacancies that remain unreacted.

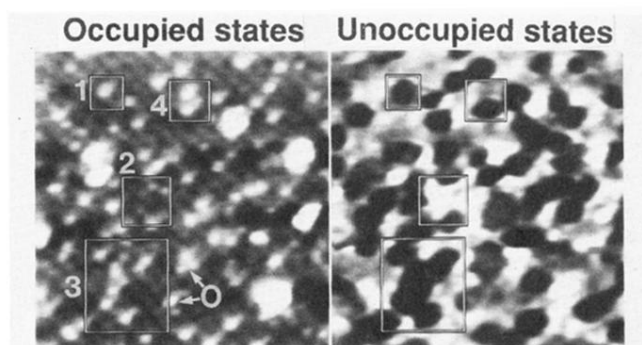


FIG. 3. Simultaneously acquired images of the occupied states and the unoccupied states of the saturated surface (sample bias ± 2.6 V, $150 \times 150 \text{ \AA}^2$). The absence of atomic resolution in the unoccupied-state image implies that the empty Si—H and Si—OH states are delocalized. The dark depressions in the unoccupied-state image correspond to the O or oxide features in the occupied-state image. The abrupt transition between light and dark areas may represent electron trapping sites around the oxide features.